Kinematics, Chaos and Fluid Deformation

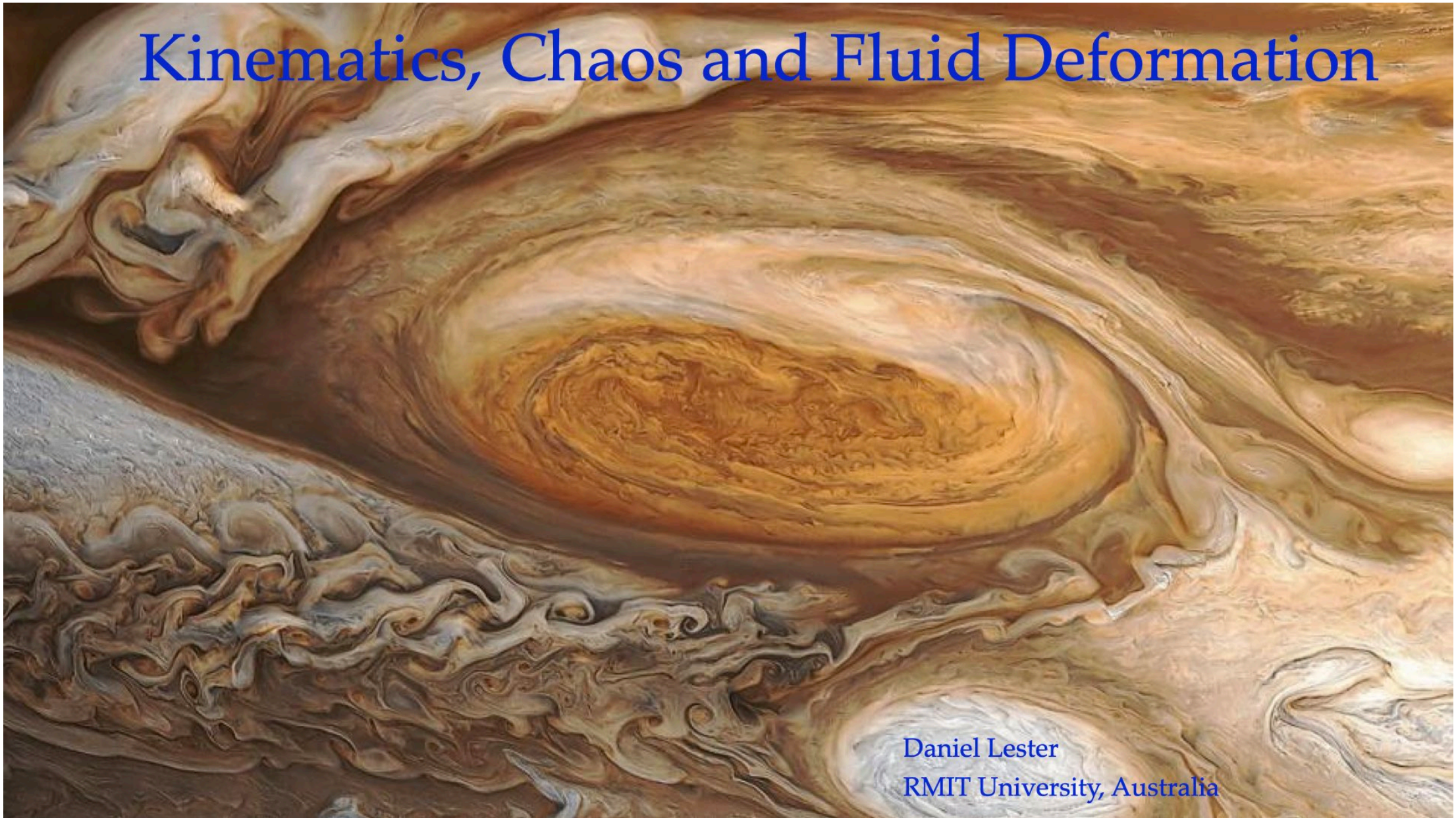

Daniel Lester
RMIT University, Australia

Outline

1. Fluid Mixing and Transport
2. Lagrangian Chaos
3. Chaos in Porous Media Flow
4. Classification of Lagrangian Kinematics
5. General Framework for Fluid Deformation
6. Deformation in Steady Porous Media Flow
7. Deformation in Unsteady Porous Media Flow
8. Summary

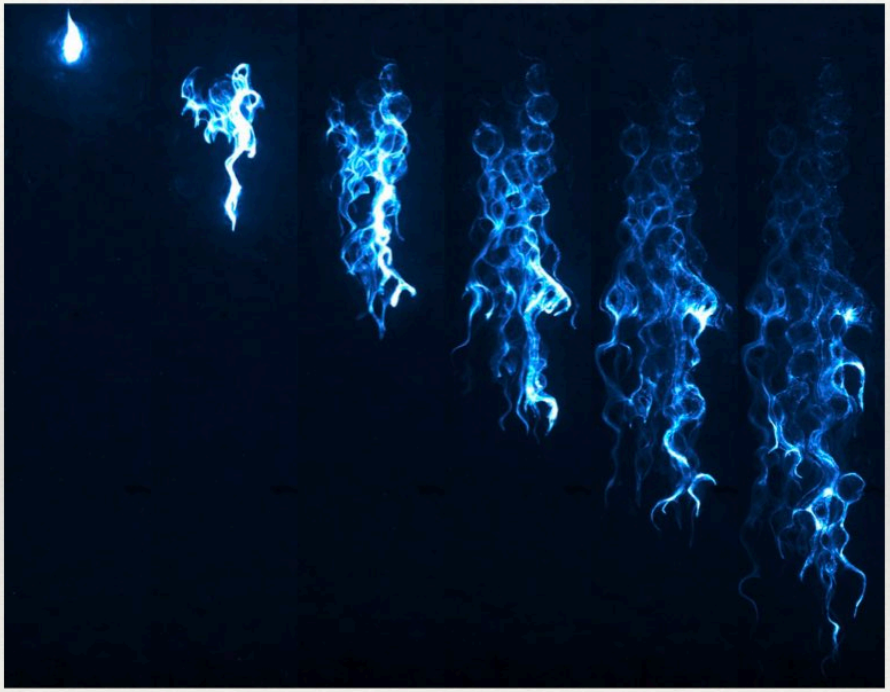

Fluorescent tracers evolving in a glass bead pack https://mathieusouzy.wordpress.com

1. Fluid Mixing and Transport

Fluid Mixing & Transport

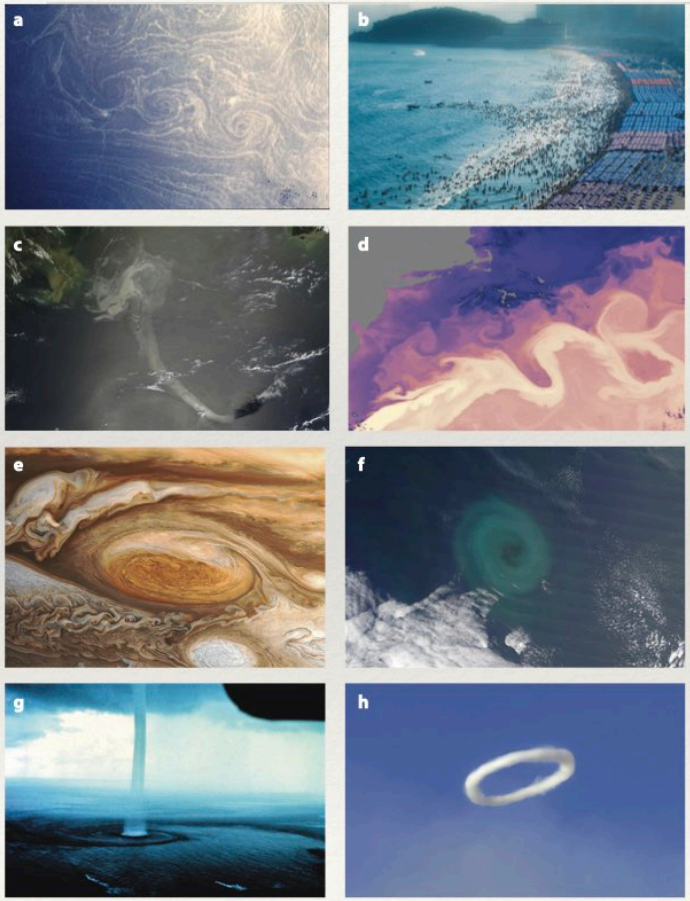

- Fluid transport and mixing governs many processes across a vast range of length scales and dynamical regimes:
- Fluid mixing is concerned with homogenisation of species concentrations
- Fluid transport is concerned with where fluid-borne species move to with time
- Both processes can be complex and require a deep understanding of flow structure in the Lagrangian frame

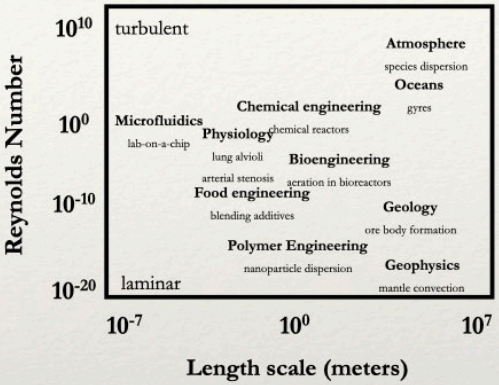

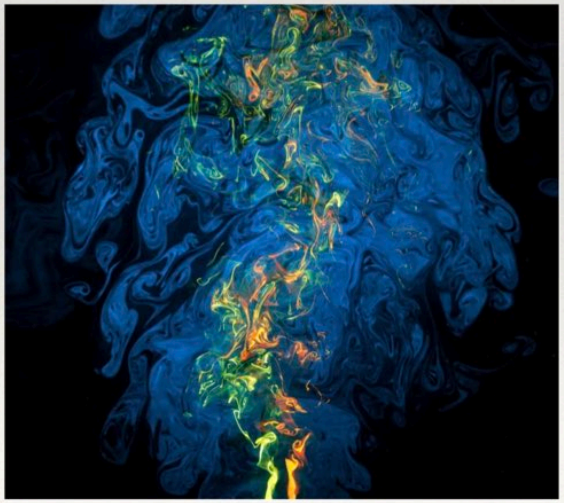

Fluid mixing and transport structures Haller, Ann. Rev. Fluid Mech. (2015)

Mixing of Spaced Jets Kree and Villermaux, Phys. Fluids (2013)

Solute Mixing

- Solute mixing arises from interplay of *stirring* and *diffusion*:

Advection-Dispersion Equation (ADE): $$\frac{\partial c}{\partial t} + \nabla \cdot (\mathbf{v}c) = \nabla \cdot (\mathbb{D}_0 \cdot \nabla c)$$

molecular diffusion: $$\mathbb{D}_0 = D_m \mathbf{1}$$

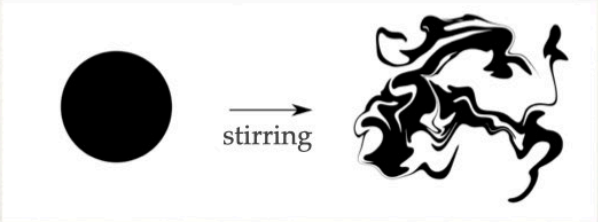

- Stirring is quantified by fluid *deformation*: stretching, shearing, folding, - can be complex and challenging to quantify

- Diffusion is easily quantified via e.g. Péclet number $Pe = \frac{LV}{D_m}$
- Diffusion occurs over time - hence deformation *history* governs mixing

Ranz, AIChE J. (1979), Villermaux, Ann. Rev. Fluid Mech. (2019)

- Once characterised, fluid deformation can be used to predict mixing (for broad Pe) via e.g. lamellar mixing theory for steady 2D Darcy flow:
- These models quantify evolution of solute concentration PDF $p_c(c)$

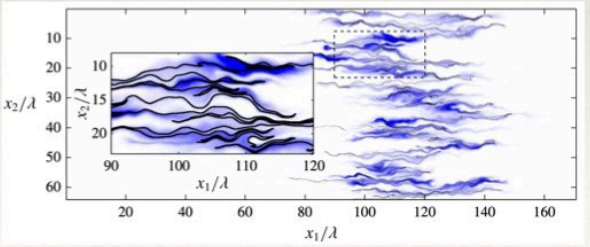

Solute mixing in steady 2D Darcy flow: LeBorgne et al, Phys. Rev. Lett. (2013), J. Fluid Mech. (2015)

Solute Transport

- Solute transport also arises from *advection* and *diffusion* - where do solute particles go with time?

$$\frac{\partial c}{\partial t} + \nabla \cdot (\mathbf{v}c) = \nabla \cdot (\mathbb{D}_0 \cdot \nabla c)$$

- Advective dynamics defines *Lagrangian topology* upon which diffusion plays out:

- Advection equation defines transform $\mathbf{\Phi}$ from Eulerian $\mathbf{x}$ to Lagrangian $\mathbf{X}$ coordinates:

$$\frac{d\mathbf{x}}{dt} = \mathbf{v}(\mathbf{x}(\mathbf{X}, t), t), \quad \mathbf{x}(\mathbf{X}, 0) = \mathbf{X} \qquad \text{Flow map:} \quad \mathbf{x}(t, \mathbf{X}) = \mathbf{\Phi}_0^t(\mathbf{X})$$

- Lagrangian topology uncovers transport barriers that hinder diffusive transport, identifies mixing/non mixing regions - crucial for understanding transport and mixing

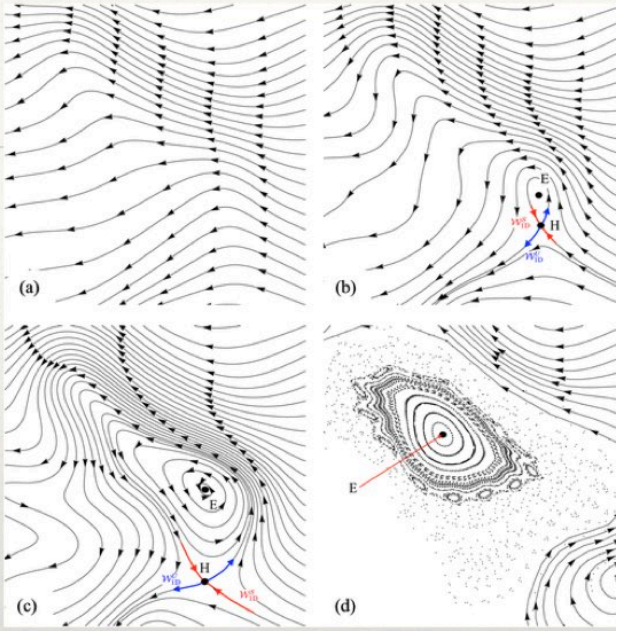

Lagrangian topology of fluid particle evolution in coastal aquifer model
Wu et al, Wat. Resour. Res. (2019)

Singular and Tensorial Mixing

- ADE is *singular* - limit of vanishing dispersivity $\neq$ zero dispersivity: $\frac{\partial c}{\partial t} + \nabla \cdot (\mathbf{v}c) = \nabla \cdot (\mathbb{D}_0 \cdot \nabla c)$

  Scalar dissipation rate $\chi := \frac{d}{dt}\langle c^2 \rangle = 2D_0 \langle (\nabla c)^2 \rangle$

  - For non-chaotic mixing: $\lim_{\mathbb{D}_0 \to 0} \chi = 0$
  - For chaotic mixing: $\lim_{\mathbb{D}_0 \to 0} \chi = \text{constant} > 0$

  Cerebelli et al, Eur. Phys. J. (2017)

- Chaotic mixing *fundamentally* alters solute mixing and dispersion (also bio/chemical reactions etc)

  Aref et al, Rev. Mod. Phys. (2017)

- Solute mixing and transport is *tensorial* - for some flows there exist distinct longitudinal and transverse components:

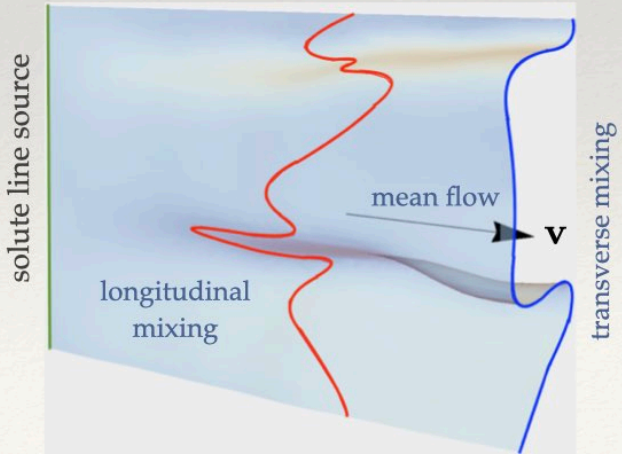

Deformation Gradient Tensor

- Deformation gradient tensor $\mathbf{F}$ quantifies transform from Eulerian $\mathbf{x}$ to Lagrangian $\mathbf{X}$ coordinates:

$$\mathbf{dx} = \mathbf{F}(\mathbf{X}, t) \cdot \mathbf{dX}$$

$$\nabla \cdot \mathbf{v} = 0 \Rightarrow \det \mathbf{F} = 1$$

- Deformation encoded to 1st order - stretching, rotation, shear, but not 2nd order - folding, twisting, etc:

$$\mathbf{v}(\mathbf{x}, t) = \mathbf{v}(\mathbf{X}, t) + \nabla_{\mathbf{X}} \mathbf{v}(\mathbf{X}, t) \cdot (\mathbf{x} - \mathbf{X}) + \dots$$

- Deformation tensor evolves according to velocity gradient:

$$\frac{\mathrm{d}\mathbf{F}}{\mathrm{dt}} = \boldsymbol{\epsilon}(t) \cdot \mathbf{F}(\mathbf{X}, t), \quad \boldsymbol{\epsilon}(t) \equiv \nabla \mathbf{v}(\mathbf{x}(\mathbf{X}, t), t)^\top$$

- As $\mathbf{F}(\mathbf{X}, t)$ is tensorial it captures both longitudinal and transverse deformation:

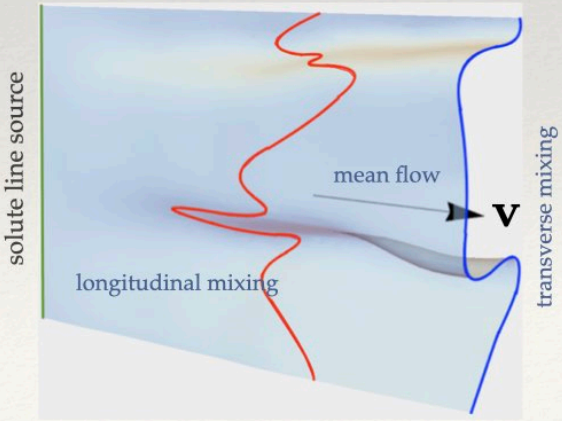

Deformation in Simple Flows

- For steady linear 2D flow types - characterised by $\det(\nabla \mathbf{v})$ - the deformation tensor at the stagnation point has analytic solutions:

rotational flow - elliptic

$\det(\nabla \mathbf{v}) > 0$

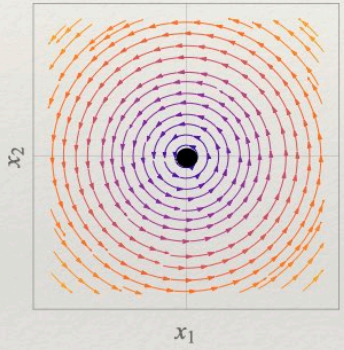

$$\mathbf{v}(\mathbf{x}) = (-x_2, x_1) \Rightarrow \nabla \mathbf{v} = \begin{pmatrix} 0 & -1 \\ 1 & 0 \end{pmatrix}$$

$$\mathbf{F}(t) = \begin{pmatrix} \cos t & \sin t \\ -\sin t & \cos t \end{pmatrix}, \quad ||\mathbf{F}|| \sim 1$$

shear flow - parabolic

$\det(\nabla \mathbf{v}) = 0$

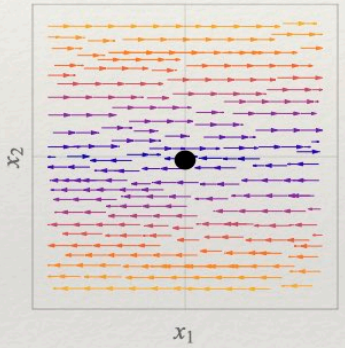

$$\mathbf{v}(\mathbf{x}) = (x_2, 0) \Rightarrow \nabla \mathbf{v} = \begin{pmatrix} 0 & 1 \\ 0 & 0 \end{pmatrix}$$

$$\mathbf{F}(t) = \begin{pmatrix} 1 & 0 \\ t & 1 \end{pmatrix}, \quad ||\mathbf{F}|| \sim t$$

saddle flow - hyperbolic

$\det(\nabla \mathbf{v}) < 0$

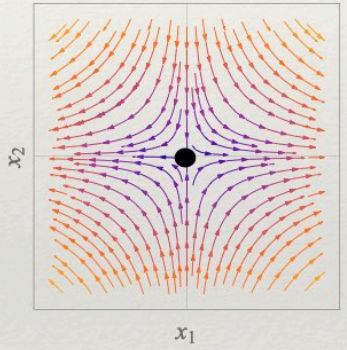

$$\mathbf{v}(\mathbf{x}) = (x_1, -x_2) \Rightarrow \nabla \mathbf{v} = \begin{pmatrix} 1 & 0 \\ 0 & -1 \end{pmatrix}$$

$$\mathbf{F}(t) = \begin{pmatrix} e^t & 0 \\ 0 & e^{-t} \end{pmatrix}, \quad ||\mathbf{F}|| \sim e^t$$

- stagnation point

- Flow types have very different deformation characteristics, ranging from zero deformation to linear to exponential in time

Deformation History Controls Mixing

- Consider a 2D or 3D Gaussian solute blob with position $\mathbf{x}_0(t)$ and covariance matrix $\mathbf{\Sigma}(t)$:

$$c(\mathbf{x},t) = \frac{c_0}{\sqrt{(2\pi)^n \det \mathbf{\Sigma}(t)}} \exp\left(-\frac{1}{2}(\mathbf{x}-\mathbf{x}_0(t))^\top \cdot \mathbf{\Sigma}^{-1}(t) \cdot (\mathbf{x}-\mathbf{x}_0(t))\right)$$

- From ADE, covariance evolves as $\mathbf{\Sigma}(t) \equiv \mathbf{\Delta}(t) + 2\mathbf{\Lambda}(t)$, valid for $||\mathbf{\Sigma}(t)|| < \ell$

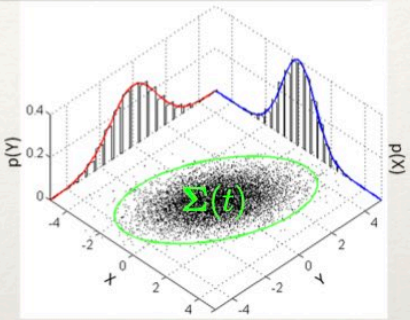

https://www.youtube.com/watch?v=_dbnH-BBSNo

blob deformation (*reversible*): $\mathbf{\Delta}(t) = \mathbf{F}(t) \cdot \mathbf{\Sigma}_0 \cdot \mathbf{F}(t)^\top$

blob dispersion (*irreversible*): $\mathbf{\Lambda}(t) = \mathbf{F}(t) \cdot \left(\int_0^t \mathbf{F}(t')^{-1} \cdot \mathbb{D}_0(t') \cdot \mathbf{F}(t')^{-\top} dt'\right) \cdot \mathbf{F}(t)^\top$

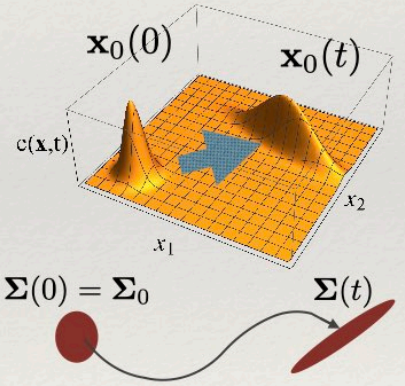

2D: Dentz et al, J. Fluid Mech. (2018)
3D: Lester et al, ArXiV (2023)

History of fluid deformation controls mixing and dispersion

ADE in Lagrangian Coordinates

- We can also cast the ADE into Lagrangian coordinate frame:

$$\frac{\partial c}{\partial t} + \nabla \cdot (\mathbf{v}c) = \nabla \cdot (\mathbb{D}_0 \cdot \nabla c) \qquad \Rightarrow \qquad \frac{\partial c}{\partial t}\Big|_{\mathbf{x}} = \nabla_{\mathbf{x}} \cdot (\mathbf{F}^{-1} \cdot \mathbb{D}_0 \cdot \mathbf{F}^{-\top} \cdot \nabla_{\mathbf{x}} c)$$

Tang & Boozer, Phys. D. (1997), Thiffeault, Phys. Lett. A (2001)

- In the Lagrangian frame, the advection term disappears, and the diffusion term becomes augmented by deformation
- Stretching and compression of fluid elements act to amplify or retard dispersion - these effects can be large
- E.g., if a material surface (in 3D) or line (in 2D) is stretching exponentially, this forms a barrier to diffusive transport:

saddle flow - hyperbolic:

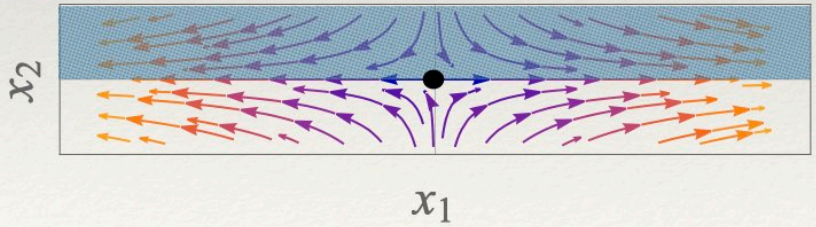

$$\mathbf{F}^{-1} \cdot (D_m \mathbf{1}) \cdot \mathbf{F}^{-\top} = D_m \begin{pmatrix} e^{2t} & 0 \\ 0 & e^{-2t} \end{pmatrix}$$

- Characterisation of $\mathbf{F}$ is key to prediction of solute mixing and transport

Fluid Advection and Flow Classes

- The remainder of this talk will focus primarily on advection - particularly Lagrangian kinematics and fluid deformation
- This approach uncovers the Lagrangian flow structure & how it impacts solute mixing and transport
- Characterisation of fluid deformation is key to prediction of fluid mixing, these serve as inputs to models of fluid mixing - see talks by Prof.s Meunier & Villermaux on Wednesday

- There exists a diverse range of flow classes, ranging from 2D to 3D, steady to unsteady, regular to chaotic, deterministic to random, laminar to turbulent - some flows are *heterogeneous* in that they contain several flow classes
- There also exist kinematic constraints such as conservation of volume, vorticity, etc
- We will develop a general toolkit to understand the Lagrangian kinematics and quantify the deformation behaviour across these diverse flow types

2. Lagrangian Chaos

Chaotic Mixing

- Advection equation is a dynamical system rich enough to admit chaos: $\frac{d\mathbf{x}}{dt} = \mathbf{v}(\mathbf{x}, t)$
- Chaotic mixing arises if d.o.f ≥ 3 (2D unsteady, 3D steady), particle trajectories form chaotic orbits
- Stretching and folding motions leads to exponential stretching: $l(t) = l(0)e^{\lambda_\infty t} \quad ||\mathbf{F}(t)|| \sim e^{\lambda_\infty t}$

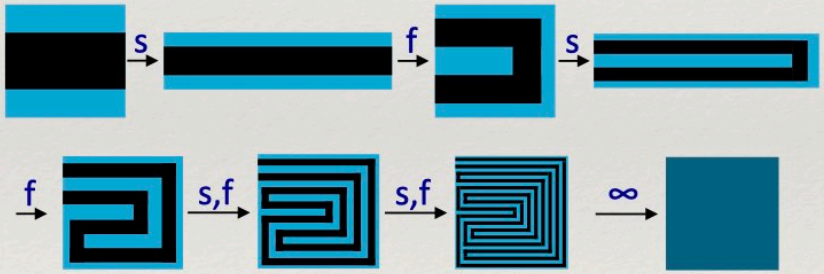

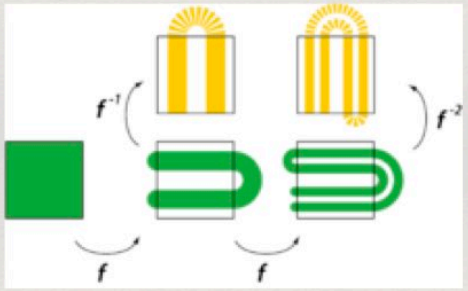

Smale horseshoe map

- Strength of chaos characterised by (infinite time) Lyapunov exponent λ_∞:

$$\lambda_i(\mathbf{X}, t) = \frac{1}{2t} \ln \sigma_i \left(\mathbf{F}(\mathbf{X}, t)^\top \cdot \mathbf{F}(\mathbf{X}, t) \right), \quad \lambda_{\infty,i} = \lim_{t \to \infty} \lambda_i(\mathbf{X}, t)$$

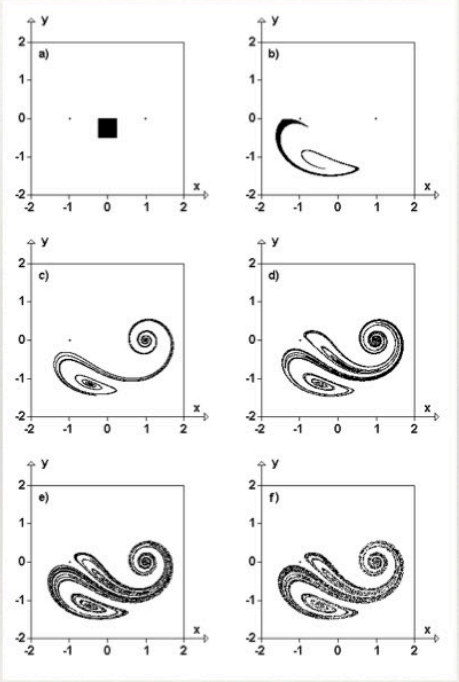

Blinking vortex flow Aref, J. Fluid Mech. (1984)

Time Periodic Sine Flow

- A simple chaotic flow is the time periodic sine flow: $\mathbf{v}^*(\mathbf{x},t) = \begin{cases} \mathbf{v}_1(\mathbf{x}) \text{ if } \mathrm{mod}(t,T) < T/2 \\ \mathbf{v}_2(\mathbf{x}) \text{ if } \mathrm{mod}(t,T) > T/2 \end{cases}$

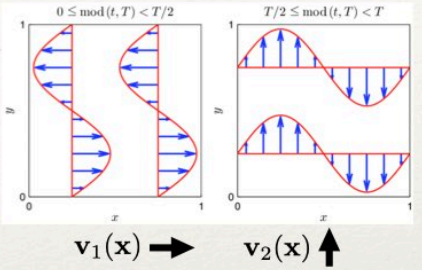

$$\mathbf{v}_1(\mathbf{x}) = (\sin 2\pi\, x_2, 0)$$
$$\mathbf{v}_2(\mathbf{x}) = (0, \sin 2\pi\, x_1)$$

- Impact of flow period T:

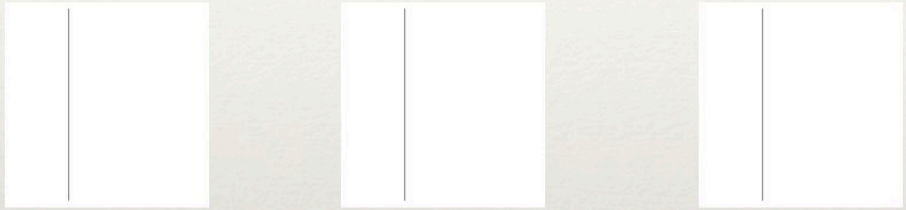

$T = 0.1$ $T = 0.2$ $T = 0.4$

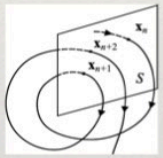

- Poincaré section S is formed by recording particle positions at every flow period T:

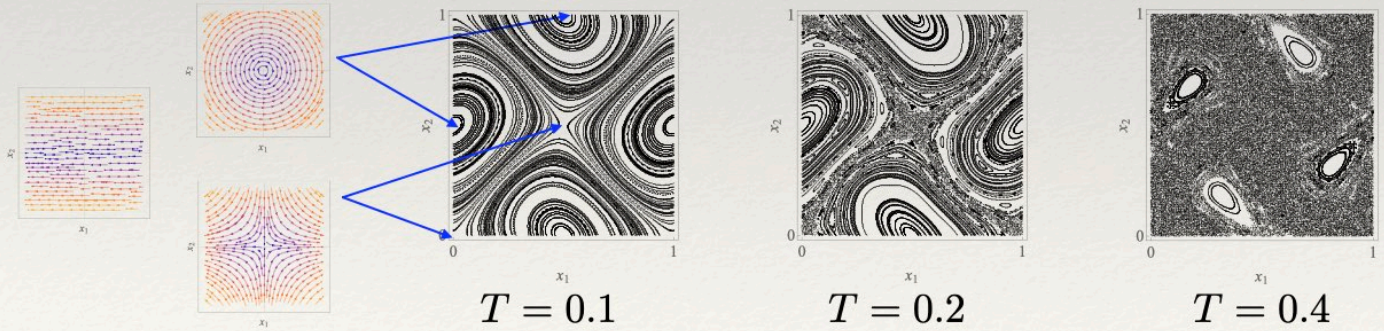

$T = 0.1$ $T = 0.2$ $T = 0.4$

For small T, flow is regular and contains elliptic, parabolic and hyperbolic structures, but at moderate T, chaotic dynamics arise…

Periodic Points

- Periodic points of degree p (defined as $\mathbf{x}_p : \mathbf{x}(\mathbf{X}, pT) = \mathbf{X},\ p = 1, 2, \ldots$) are similar to stagnation points in steady flows:

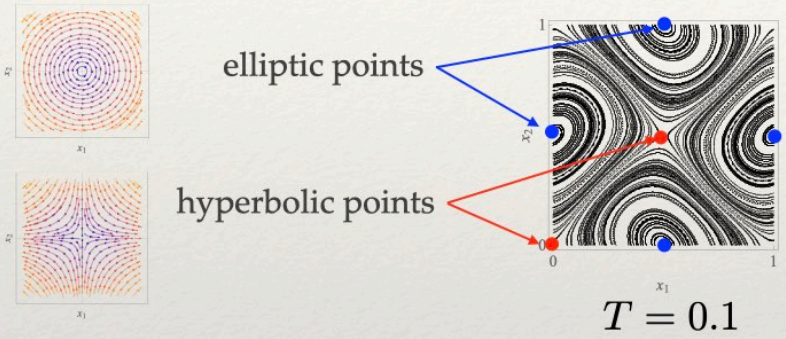

elliptic: $\mu_i = \exp(\pm i\theta)$ complex $\Rightarrow \mathbf{F}' = \begin{pmatrix} \sin\theta & \cos\theta \\ -\sin\theta & \cos\theta \end{pmatrix}$

parabolic: $\mu_i = \pm 1$ real $\Rightarrow \mathbf{F}' = \begin{pmatrix} 1 & \gamma \\ 0 & 1 \end{pmatrix}$

hyperbolic: $\mu_2 = 1/\mu_1$ real $\Rightarrow \mathbf{F}' = \begin{pmatrix} \mu & 0 \\ 0 & 1/\mu \end{pmatrix}$

- Periodic points are classified as elliptic, parabolic, hyperbolic based on eigenvalues of $\mathbf{F}$: $\mu_i = \text{eigs}[\mathbf{F}(\mathbf{x}_p, pT)]$

- Elliptic structures are transport barriers which are stable to perturbations (Kolmogorov-Arnold-Moser (KAM) theory)

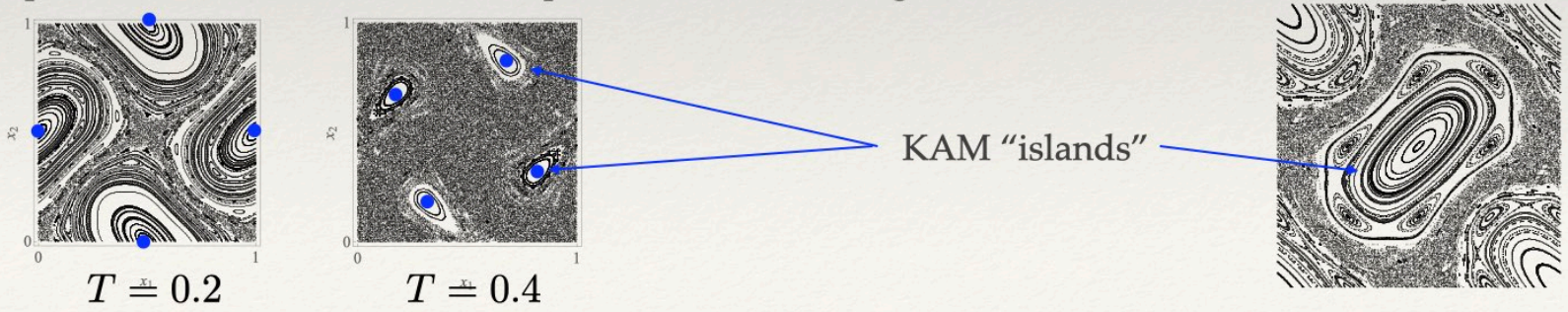

Hyperbolic Points and Manifolds

- Hyperbolic points in 2D flows contain exponentially expanding and contracting eigenvectors which extend into the flow to form 1D stable $\mathcal{W}^s_{1D}(\mathbf{x}_p)$ and unstable $\mathcal{W}^u_{1D}(\mathbf{x}_p)$ *hyperbolic manifolds* - these connect with flow boundaries or other hyperbolic points:

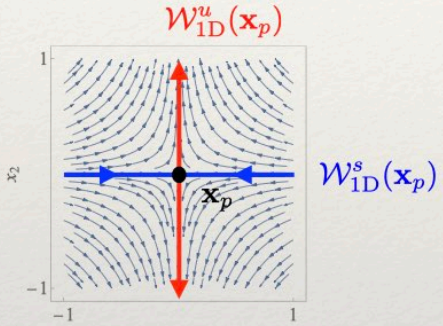

steady / periodic 2D flow

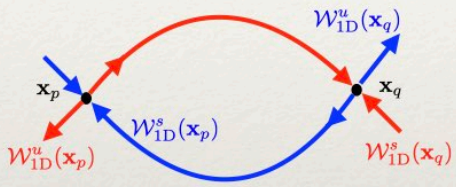

heteroclinic connection

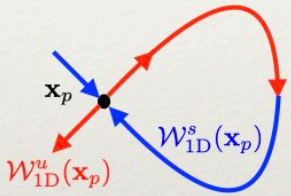

homoclinic connection

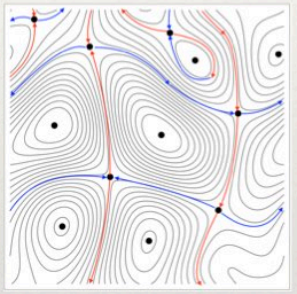
steady 2D flow

- For steady 2D flows, these connections are **always** smooth - exponential stretching along an unstable manifold is cancelled as the manifold turns into a stable one - no net exponential stretching

- Hyperbolic manifolds attract fluid particles and control transport - the manifold network forms the "skeleton" of the flow Mackay, J Nonlin. Sci. (1994)

- In steady and periodic 3D flows, stagnation / periodic points generate 1D and 2D hyperbolic manifolds - 2D manifolds control transport:

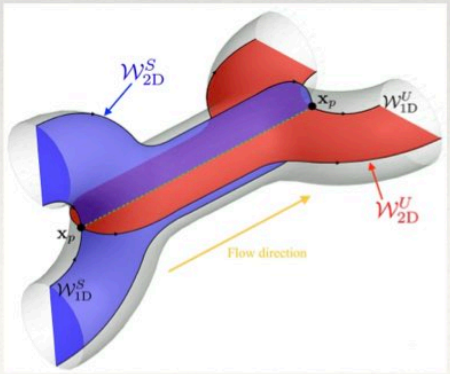

Hetero/Homoclinic Tangles

- In periodic 2D flows and steady or periodic 3D flows, smooth hetero/homoclinic connections may not occur…

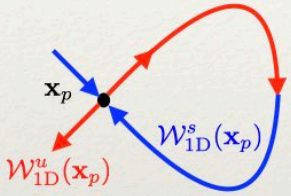

homoclinic connection

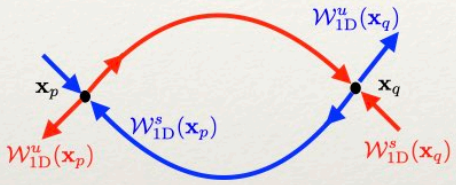

heteroclinic connection

- If manifolds cross, an infinite number of crossings must occur, leading to a heteroclinc or homoclinic *tangle*:

Poincaré (1899): *"When we try to represent the figure formed by [the stable and unstable manifolds] and their infinitely many intersections … [the manifolds must] bend back upon itself in a very complex manner in order to cut across all of the meshes in the grid an infinite number of times."*

- This generates exponential stretching and folding of fluid elements, leading to a chaotic scattering of points:

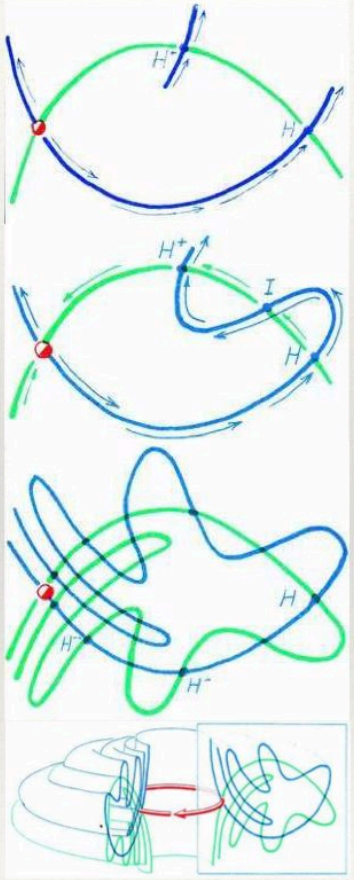

Homoclinic Tangle Abraham and Shaw, Dynamics: The Geometry of Behaviour (1992)

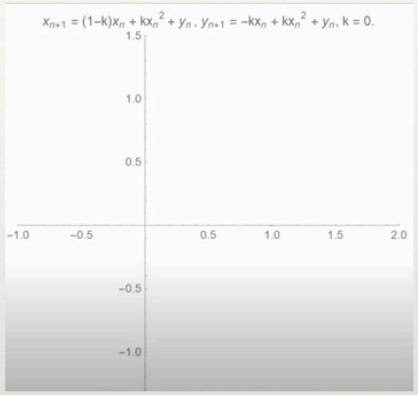

https://www.youtube.com/shorts/mSU1S058ssE?feature=share

Lagrangian Topology

- Nonlinear dynamics of fluid advection facilitates insight into Lagrangian topology (flow structure):

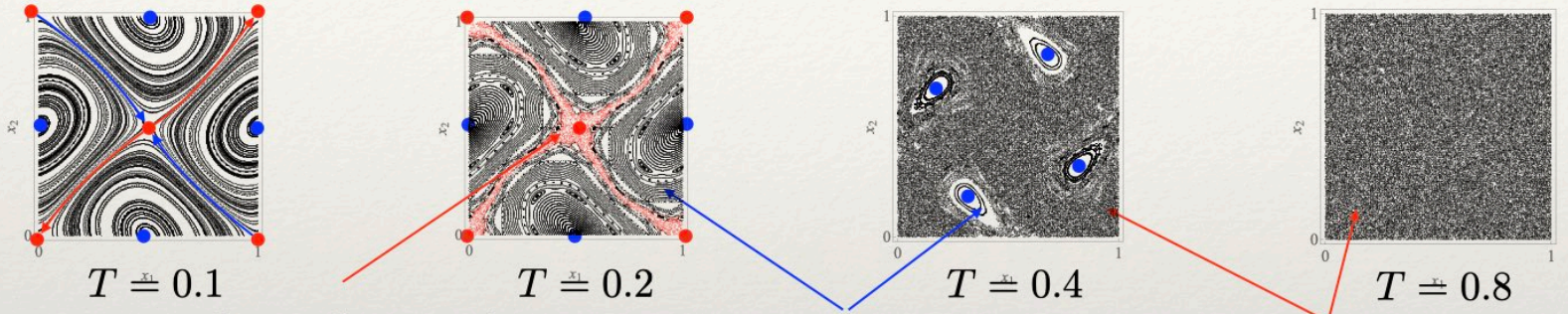

- Lagrangian topology is divided into distinct chaotic (mixing) and regular (non-mixing) regions

- Similar concepts apply in 3D:

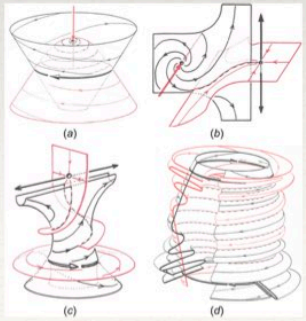

Heteroclinic tangles in 3D Abraham and Shaw, Dynamics: The Geometry of Behaviour (1992)

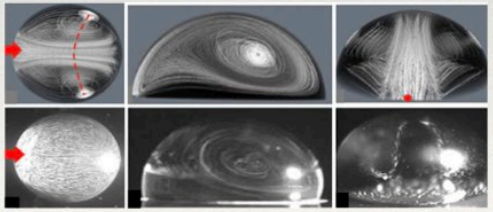

Alghane et al, J. Appl. Phys. (2011)

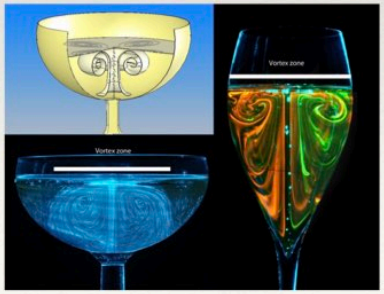

Polidori et al, J. Visualiz. (2008)

Lagrangian Coherent Structures

- Classical dynamical systems does not apply to aperiodic flows - periodic points etc do not exist
- But *Lagrangian Coherent Structures* (LCS) exist that control transport and mixing…
- Hyperbolic, elliptic and parabolic LCSs are defined respectively as the most attracting / repelling, non-stretching and non-shearing surfaces (lines) in 3D and 2D flows
- One* detection method is via ridges of the FTLE field: $\lambda_i(\mathbf{X},t) = \frac{1}{2t}\ln\sigma_i\left(\mathbf{F}(\mathbf{X},t)^\top \cdot \mathbf{F}(\mathbf{X},t)\right)$

  *Hadjighasem et al, Chaos (2017)

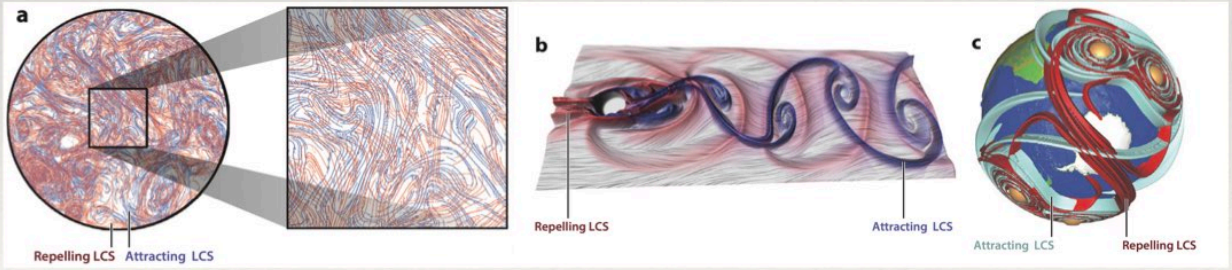

(a) rotating 2D turbulence, (b) Von Karman vortex street, (c) geophysical transport. Haller, Ann. Rev. Fluid Mech. (2015)

- Repelling [red] (attracting [blue]) LCS are ridges of forward (backward) in time FTLEs

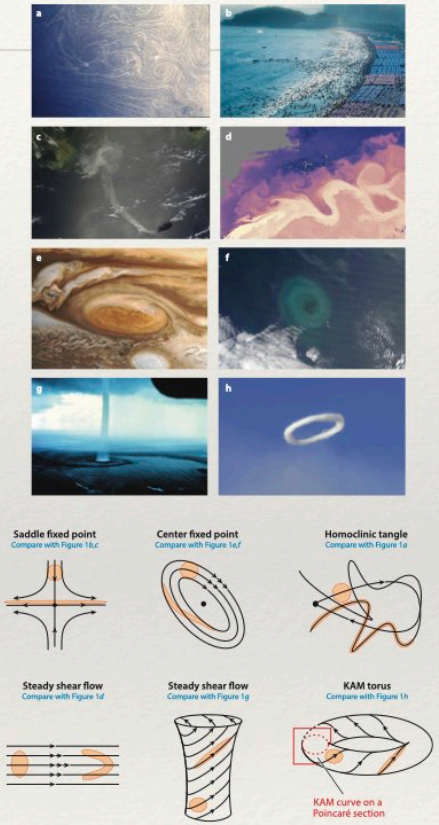

(Top) coherent Lagrangian patterns in nature, (bottom) equivalent classical dynamics flow structures. Haller, Ann. Rev. Fluid Mech. (2015)

Hyperbolic, Elliptic and Parabolic LCS

- Backward in time FTLE field for vortex shedding from flat plate at 35°, Re=100:

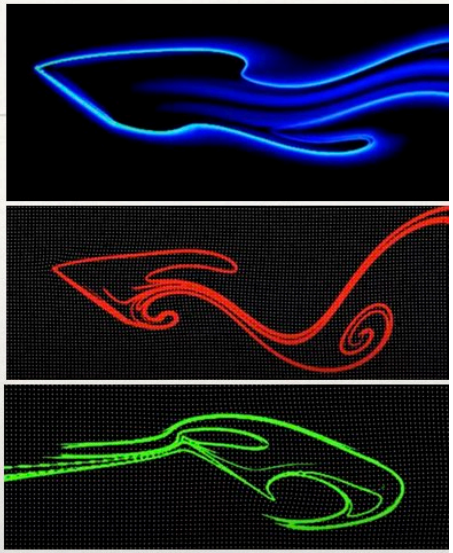

Brunton and Rowley, Chaos (2010)

Hyperbolic LCS attract and repel particles:

- Fluid particles are attracted to and bound by back-in-time FTLE ridges:
- Fluid particles are repelled from and bound by forward-in-time FTLE ridges:

Elliptic LCS are closed surfaces with zero stretching:

Parabolic LCS are surfaces with minimal stretching or shear:

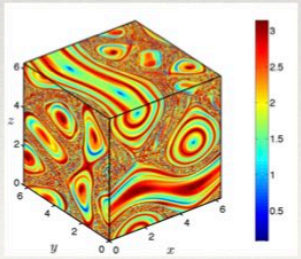

Elliptic LCS in ABC flow
Farazmad and Haller, Physica D (2016)

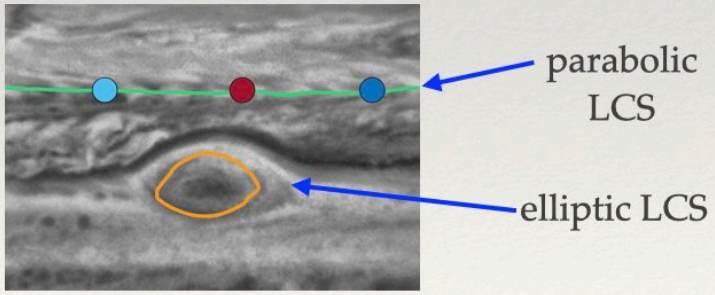

LCS around Jupiter's Red Spot
Hadjighasem and Haller, SIAM Rev. (2016)

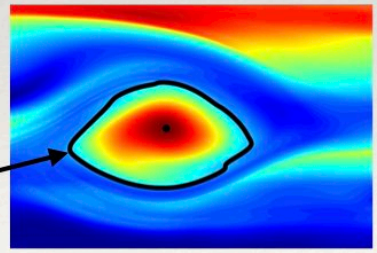

LCS around Jupiter's Red Spot
Hadjighasem et al, Chaos (2017)

Streamline Braiding

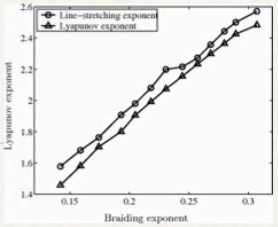

Lyapunov exponent from braiding
Thiffeault, Phys. Rev. Lett. (2005)

- In steady & unsteady flows, chaotic trajectories manifest as braiding stream / path lines
- If streamlines braid non-trivially, fluid elements are stretched exponentially
- Lyapunov exponent λ_∞ can be estimated from braiding motions
- Braiding streamlines are observed in many pore and Darcy scale flows:

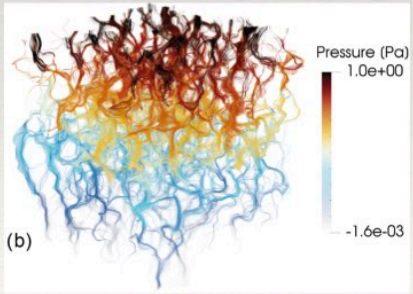

Porescale flow
Eichheimer et al, Solid Earth (2019)

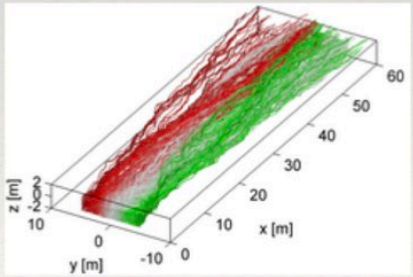

Anisotropic Darcy flow
Cirpka et al, Wat. Resour. Res. (2015)

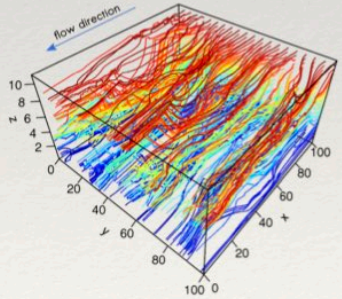

Anisotropic Darcy flow
Huber et al, Hydrol. Earth Syst. Sci (2016)

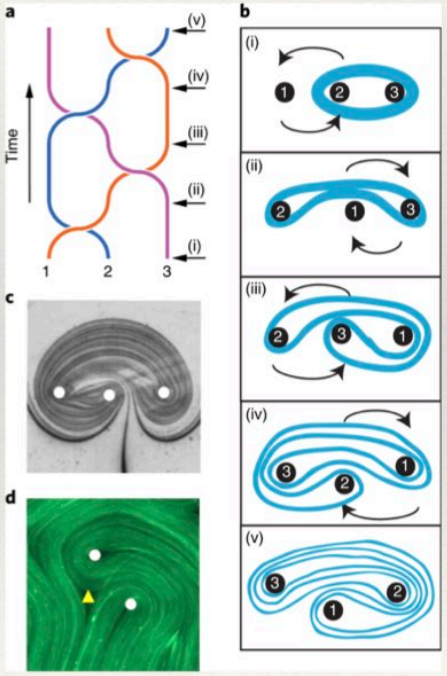

Braiding in nematic liquid crystals
Tan et al, Nature Phys. (2019)

Helicity and Streamfunctions

- Helicity density h measures complexity of flow topology - if h=0, flow is *integrable* (non-chaotic):

Moffatt, J. Fluid Mech. (1969)
Moreau, Comptes Rendus (1961)

$$h \equiv \mathbf{v} \cdot (\nabla \times \mathbf{v})$$

- All steady 2D flows are helicity-free, and some steady 3D flows (e.g. isotropic Darcy flow) are helicity-free:

$$\mathbf{v} = -k\nabla\phi \Rightarrow h = k\nabla\phi \cdot (\nabla\phi \times \nabla k) = 0$$

- 3D helicity-free flows admit a pair of streamfunctions:

Yoshida, J. Math. Phys. (2009)

$$\mathbf{A} = \sum_{i=1}^{N} \alpha_i \nabla\beta_i, \quad N = 1 \text{ if } h = 0$$

$$\mathbf{v} = \nabla \times \mathbf{A} = \nabla\psi_1 \times \nabla\psi_2$$

- Streamfunctions constrain Lagrangian kinematics (no braiding), prohibit mixing and transverse macrodispersion - is this representative of real porous media?

Lester et al, J. Fluid Mech. (2021, 2022), Wat. Resour. Res. (2023)

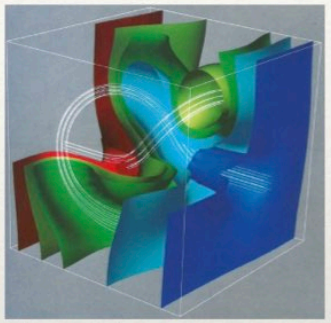

Helical anisotropic Darcy flow
Cole and Foote, Dyn. Fluid Hier. Porous Media (1990)

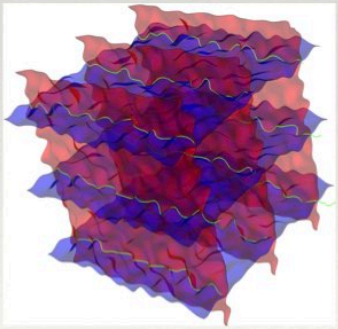

Helicity-free isotropic Darcy flow
Lester et al, J. Fluid Mech. (2021)

3. Chaos in Porous Media Flows

Steady Pore-Scale Flow

- Steady 3D pore-scale flows are inherently chaotic
- Granular media and pore networks have complex pore-scale topology ($g \gg 0$) which admit stagnation points at pore junctions - these generate heteroclinic tangles:
  Lester et al, Phys. Rev. Lett. (2013), J. Fluid Mech. (2016)
- Fluid elements are stretched and folded during advection - strong link with grain structure
  Turuban et al, Phys. Rev. Lett. (2018), J. Fluid Mech. (2019)

$$\chi = 2(1-g) = \sum \gamma_p(\mathbf{x}_p) \ll 0$$

$\chi \ll 0$: Euler characteristic

$g \gg 0$: topological genus

$\gamma_p = -1$: saddle point

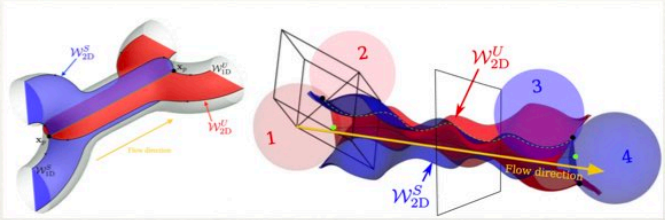

Lester et al, submitted, Phys. Rev. X (2023)

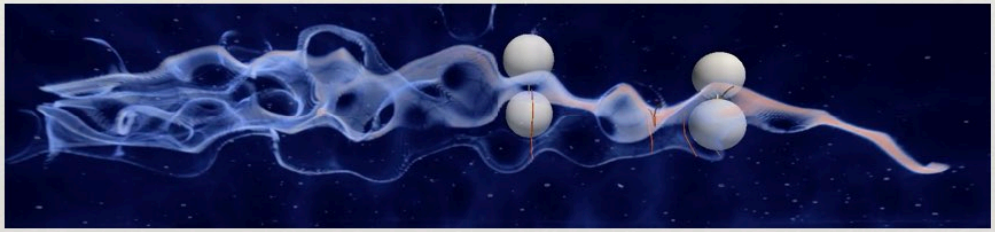

Solute mixing in glass beadpack: Heyman et al, PNAS (2020)

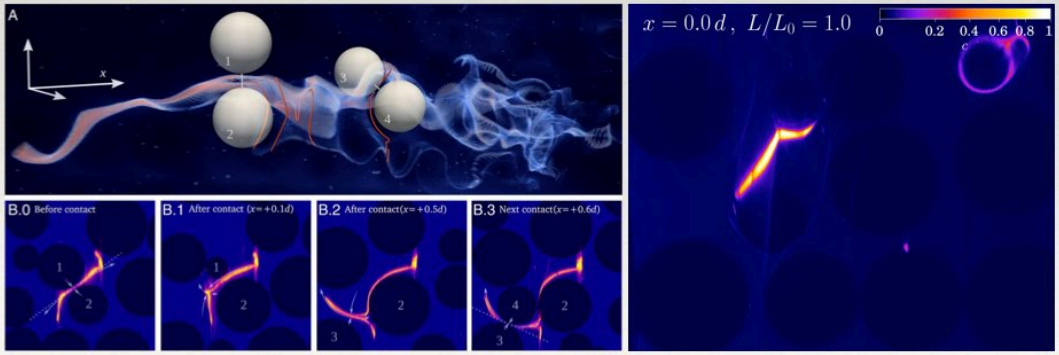

Stretching and folding in glass beadpack: Heyman et al, PNAS (2020)

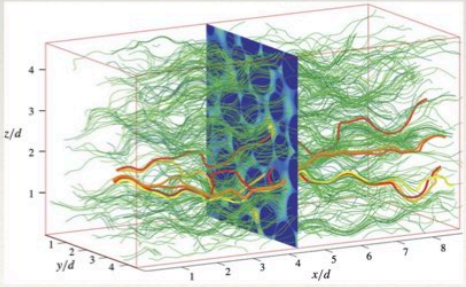

Reconstructed streamlines from PIV: Souzy et al, J. Fluid Mech. (2020)

Unsteady Pore-Scale Flow

- "Push-pull" flow generates complex solute distributions, despite net zero fluid deformation
- Highly heterogeneous and anisotropic dispersion results - "diffusive signature" of chaotic pore-scale flow
- Analysis of solute dispersion allows characterisation of chaotic mixing at pore scale

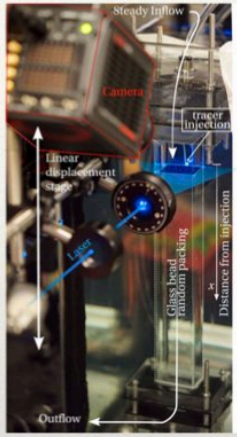

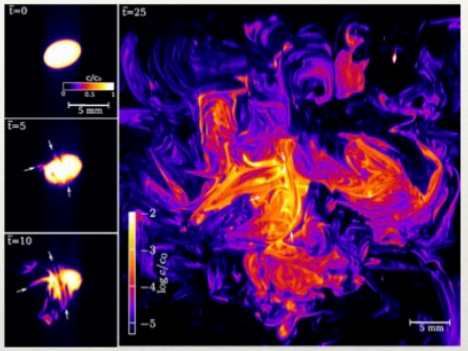

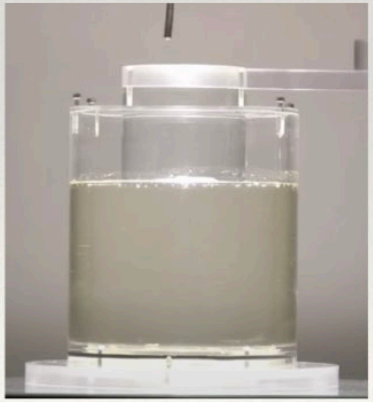

push-pull analogue

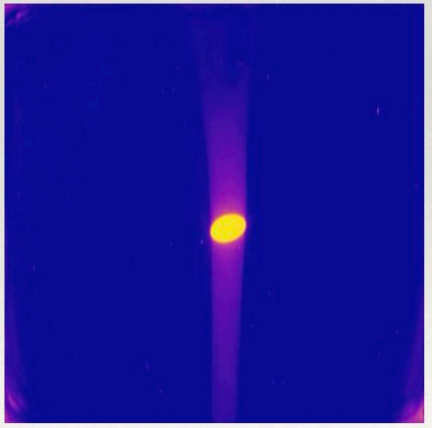

Push-pull mixing in glass beadpack:
Heyman et al, Phys. Rev. Lett (2021)

Steady Darcy Flow

- Steady Darcy flow in 3D isotropic porous media exhibits zero transverse macrodispersion - is this realistic?
- Steady Darcy flow in 3D anisotropic porous media can generate non-zero helicity:

$$\mathbf{v}(\mathbf{x}) = -\mathbf{K}(\mathbf{x}) \cdot \nabla\phi(\mathbf{x}), \quad h(\mathbf{x}) = \mathbf{v}(\mathbf{x}) \cdot \nabla \times \mathbf{v}(\mathbf{x}) \neq 0$$

- Non-stationary conductivity drives strong fluid braiding and apparent chaotic mixing:
- Accelerated solute mixing observed numerically and experimentally:
- Is chaotic mixing ubiquitous at the Darcy scale?

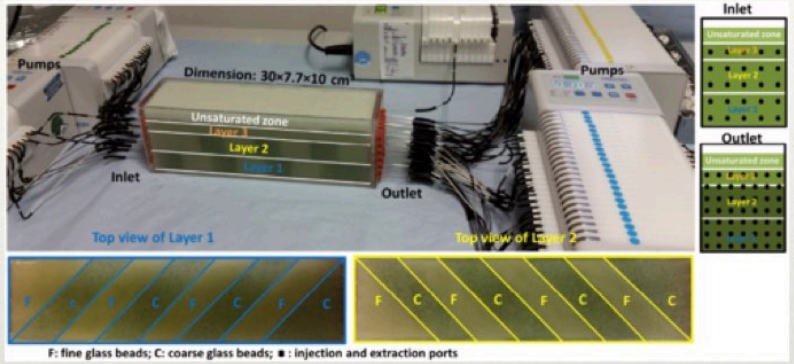

Helical flow in layered porous media: Ye et al, Phys. Rev. Lett. (2015)

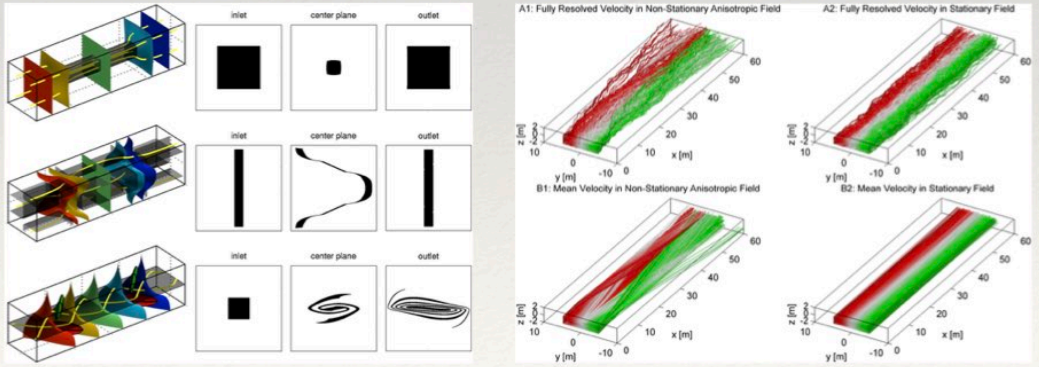

Mixing in anisotropic Darcy flow: Cirpka et al, Wat. Resour. Res. (2015), Chignoa et al, Wat. Resour. Res.(2015)

Unsteady Darcy Flow

- Engineered Darcy flows can generate chaotic mixing:
- Natural systems involving compressible media + transient forcing lead to complex dynamics
- Heterogeneous Lagrangian topology consists of mixing and non-mixing regions:

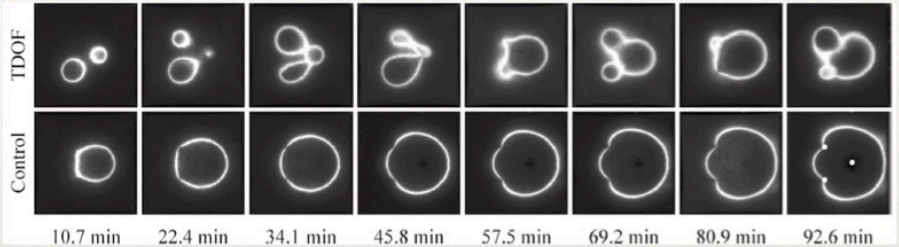

Enhanced mixing and reaction in transient Darcy flow: Zhang et al, Env. Sci. Tech. (2019)

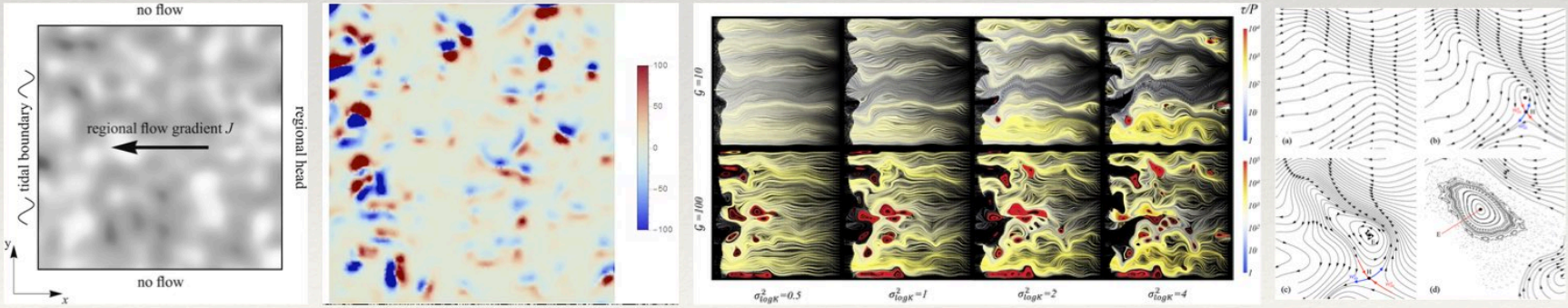

Mixing in oscillatory Darcy flow: Trefry et al, Wat. Resour. Res.(2019), Wu et al, Wat. Resour. Res. (2019), Trefry et al, TIPM (2020)

4. Classification of Lagrangian Kinematics

Classification of Lagrangian Kinematics

Increasing kinematic constraints

Increasing kinematic complexity

	dimensionality	helical	chaotic	examples	"simple" kinematics
Steady	2D	x	x	2D pore, Darcy scale flow	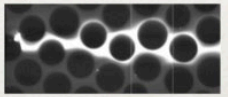
	3D	x	x	3D isotropic Darcy flow	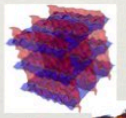
	3D	√	√	3D pore, anisotropic Darcy flow	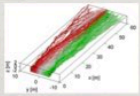 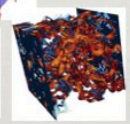
Unsteady	2D	-	√	2D pore, Darcy flow	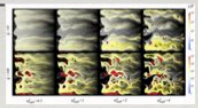
	3D	-	√	3D pore, Darcy flow	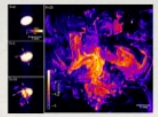

"complex" kinematics

Q: How to properly quantify the Lagrangian kinematics of these diverse flows?

5. General Framework for Fluid Deformation

Deformation in Protean Coordinates

- In a moving & rotating coordinate frame $\mathbf{x}' = \mathbf{Q}(t) \cdot (\mathbf{x} - \mathbf{x}_0(t))$, both $\boldsymbol{\epsilon}'(t)$ and $\mathbf{F}'(t)$ are upper triangular:

off-diagonal terms quantify shear, diagonal terms quantify stretching

$$\boldsymbol{\epsilon}'(t) = \begin{pmatrix} \epsilon'_{11} & \epsilon'_{12} & \epsilon'_{13} \\ 0 & \epsilon'_{22} & \epsilon'_{23} \\ 0 & 0 & \epsilon'_{33} \end{pmatrix} \quad \Rightarrow \quad \frac{d\mathbf{F}'}{dt} = \boldsymbol{\epsilon}'(t) \cdot \mathbf{F}'(t) \quad \Rightarrow \quad \mathbf{F}'(t) = \begin{pmatrix} F'_{11} & F'_{12} & F'_{13} \\ 0 & F'_{22} & F'_{23} \\ 0 & 0 & F'_{33} \end{pmatrix}$$

- Deformation tensor **much** simpler to solve: $F'_{ii}(t) = \exp\left(\int_0^t \epsilon'_{ij}(t')dt'\right)$ $F'_{ij}(t) = \int_0^t f(\epsilon'_{ij}(t'), F'_{\alpha\beta<ij}(t'))dt'$
- Lyapunov exponents: $\lambda_{\infty,i} = \langle \epsilon'_{ii} \rangle$

- For steady flows, Protean coords are streamline coords:
- For *h*-free flows, Protean coords are streamfunctions:

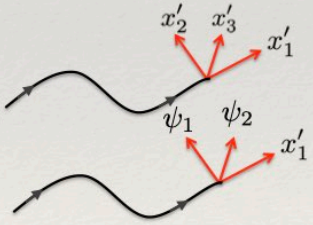

- For unsteady flows, streamlines don't exist, Protean coords "tumble":

For steady flows, $\mathbf{F}'(t)$ quantifies longitudinal & transverse deformation:

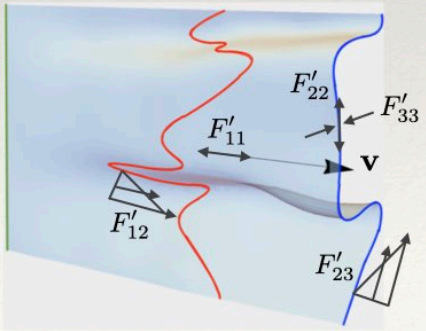

Deformation Across Flow Classes

$$\boldsymbol{\epsilon}'(t) = \left(\begin{array}{cc|c} \epsilon'_{11} & \epsilon'_{12} & \epsilon'_{13} \\ 0 & \epsilon'_{22} & \epsilon'_{23} \\ \hline 0 & 0 & \epsilon'_{33} \end{array}\right)$$

Increasing kinematic constraints

Increasing kinematic complexity

	d	helical	chaotic	# non-zero off-diagonal ϵ'_{ij}	# independent non-zero $\lambda_{\infty,i}$	$\langle F'_{11} \rangle$	$\langle F'_{22} \rangle$	$\langle F'_{33} \rangle$
Steady	2D	x	x	1	0	1	1	-
	3D	x	x	2	0	1	1	1
	3D	√	√	3	1	1	$e^{\lambda_\infty t}$	$e^{-\lambda_\infty t}$
Unsteady	2D	-	√	1	1	$e^{\lambda_\infty t}$	$e^{-\lambda_\infty t}$	-
	3D	-	√	3	2	$e^{\lambda_{\infty,1} t}$	$e^{\lambda_{\infty,2} t}$	$e^{-(\lambda_{\infty,1}+\lambda_{\infty,2})t}$

Protean velocity gradient $\boldsymbol{\epsilon}'(t)$ captures **constraints** and **complexity** of Lagrangian kinematics across all flow classes

Application to Homogeneous Flows

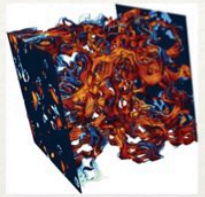

Q: How can I apply this framework to homogeneous flows?

A: Given a 2D/3D, steady/unsteady velocity field, perform parallel particle tracking to generate $\mathbf{x}_0(t)$ then rotate via $\mathbf{Q}(t)$ into Protean frame: $\mathbf{x}'(t) \equiv \mathbf{Q}(t) \cdot (\mathbf{x} - \mathbf{x}_0(t))$

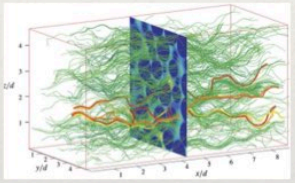

Next, determine Protean velocity gradient $\boldsymbol{\epsilon}'(t) = \mathbf{Q}^\top(t)\boldsymbol{\epsilon}(t)\mathbf{Q}(t) + \dot{\mathbf{Q}}^\top(t)\mathbf{Q}(t)$ along many path lines and gather statistics on $\boldsymbol{\epsilon}'(t)$, $v(t)$ (PDFs, correlations, etc)

- Can be applied to quite complex flows, e.g. Johns Hopkins turbulence database*:

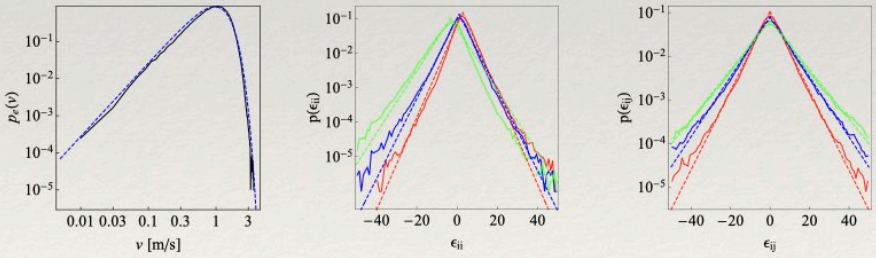

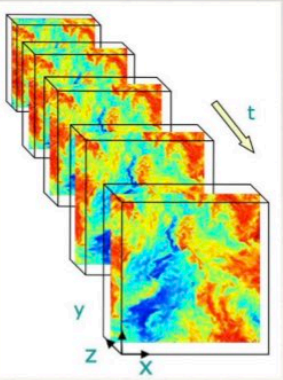

- Statistical characterisation of $\boldsymbol{\epsilon}'(t)$ facilitates prediction of $\mathbf{F}'(t)$ (and so quantifies solute mixing)

*http://turbulence.pha.jhu.edu/

Application to Heterogeneous Flows

- For flows with heterogeneous Lagrangian topology - i.e. comprised of non-mixing KAM "islands", chaotic "seas", regular regions etc:

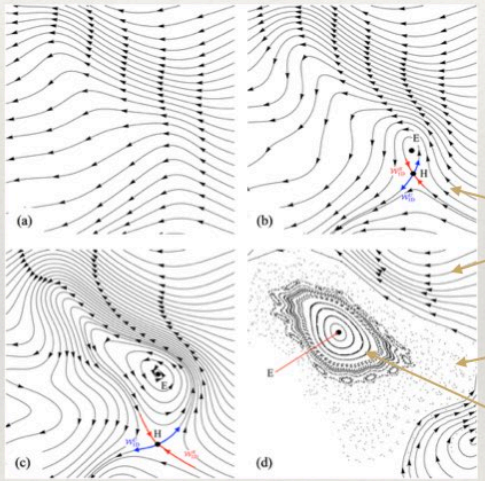

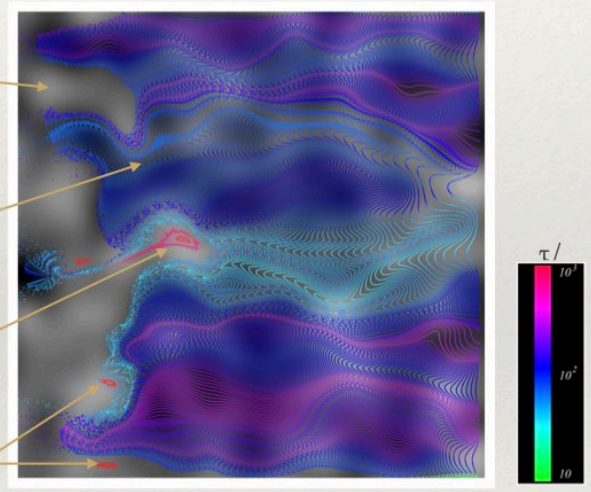

Wu et al, Wat. Resour. Res. (2019)

Trefry et al, Wat. Resour. Res.(2019)

- For these heterogeneous systems, we can quantify deformation and mixing in each sub-domain - an outstanding challenge is to develop global transport theories

6. Deformation in Steady Porous Media Flow

Fluid Deformation as a Random Walk

- Now $\boldsymbol{\epsilon}'(t)$ is characterised, we can develop an *ab initio* continuous time random walk (CTRW) for $\mathbf{F}'(t)$
- Deformation CTRW captures stochastic nature of heterogeneous media and *preserves* the underlying Lagrangian kinematics
- For steady flows, velocity (and $\boldsymbol{\epsilon}'(t)$) decorrelates with streamline distance *s*, not time:

Le Borgne et al, Phys. Rev. Lett. (2007)
Lester et al, J. Fluid Mech (2018)

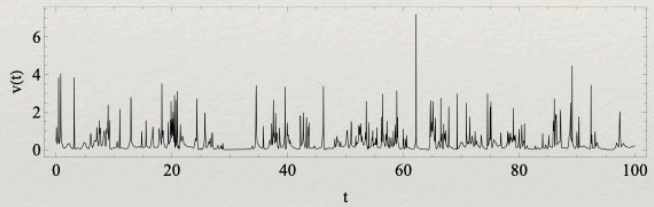

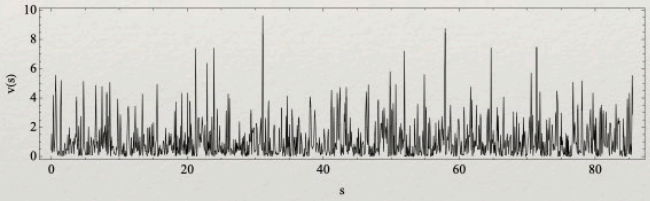

- Spatial Markovianity (with decorrelation length s_d) justifies deformation CTRW in *s*-space:

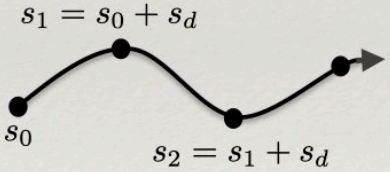

$$F'_{ij}(s) = \int_0^s \frac{f(\epsilon'_{ij}(s'), F'_{\alpha\beta<ij}(s'))}{v(s')} ds' \quad \Rightarrow \quad s_{n+1} = s_n + s_d, \quad t_{n+1} = t_n + \frac{s_d}{v_n}$$

$$F'_{ij,n+1} = F'_{ij,n} + \frac{f_n}{v_n}$$

- Closed-form solutions developed for coupled CTRW:

CTRW: Dentz et al, Phys. Rev. E (2016a)
2D: Dentz et al, Phys. Rev. E (2016b)
3D: Lester et al, J. Fluid Mech (2018)

2D Steady Darcy Flow

$$\mathbf{F}'(t) = \begin{pmatrix} F'_{11} & F'_{12} \\ 0 & F'_{22} \end{pmatrix}$$

- For 2D steady flow, only longitudinal mixing:

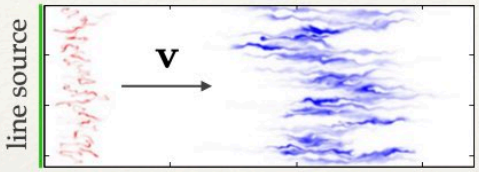

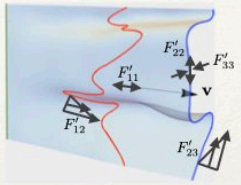

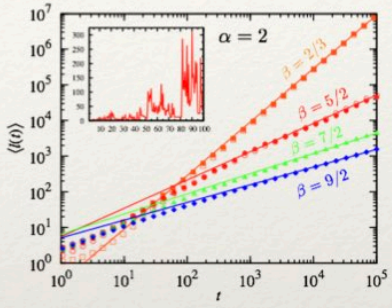

- Only $F'_{12}(s)$ component grows: $F'_{12}(s) \propto \int_0^s \frac{\epsilon'_{12}(s')}{v(s')^3} ds'$, $|\epsilon'_{12}| \propto v^{\alpha+3}$

Stretching of fluid elements: Dentz et al, Phys. Rev. E (2016a, 2016b)

- For $p_v(v) \propto v^{1-\beta}$, deformation CTRW predicts algebraic stretching:

$$\langle \ell(t) \rangle = \langle |F'_{12}(t)| \rangle \sim t^r \qquad 0 < r(\alpha, \beta) < 2$$

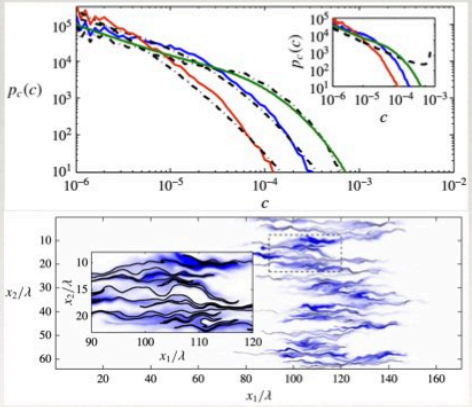

- Stretching rate *r* input parameter to lamellar mixing models for solute concentration PDF:

- No transverse macrodispersion as $\langle F'_{22} \rangle = 1$, $\langle |F'_{12}| \rangle$ quantifies longitudinal

Solute mixing: LeBorgne et al, J. Fluid Mech. (2015)
LeBorgne et al, Phys. Rev. Lett. (2013)

3D Steady Isotropic Darcy Flow

$$\mathbf{F}'(t) = \begin{pmatrix} F'_{11} & F'_{12} & F'_{13} \\ 0 & F'_{22} & 0 \\ 0 & 0 & F'_{22} \end{pmatrix}$$

- For 3D isotropic Darcy flow, zero helicity density admits dual stream functions: $\mathbf{v} = \nabla\psi_1 \times \nabla\psi_2$
- Shears decouple as $h = 0 \Rightarrow \epsilon'_{23} = 0$ and Lyapunov exponent is zero: $\boldsymbol{\epsilon}'(t) = \begin{pmatrix} \epsilon'_{11} & \epsilon'_{12} & \epsilon'_{13} \\ 0 & \epsilon'_{22} & 0 \\ 0 & 0 & \epsilon'_{33} \end{pmatrix}$

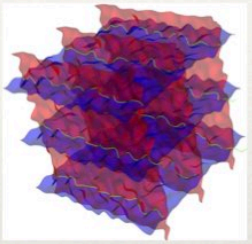

Lester et al, J. Fluid Mech. (2021)

- All diagonal components F'_{ii} simply fluctuate: $\langle F'_{ii} \rangle = 1$
- Deformation CTRW yields off-diagonal components similar to 2D flow:

$$\langle |F'_{12}| \rangle,\ \langle |F'_{13}| \rangle \sim t^r \qquad 0 < r(\alpha, \beta) < 2$$

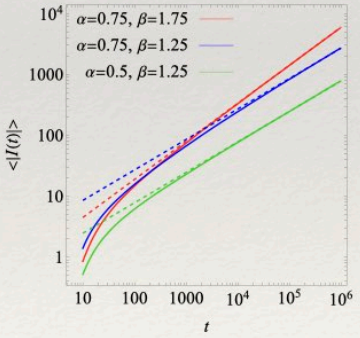

- Zero transverse macrodispersion as $\langle F'_{22} \rangle = \langle F'_{33} \rangle = 1$
  - conventional numerical schemes don't preserve this constraint

  Lester et al, Wat. Res. Res. (2023)

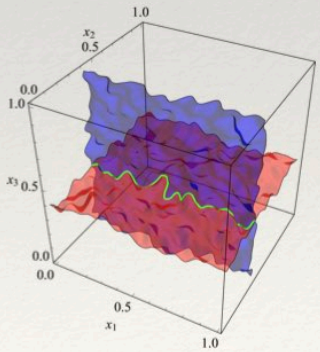

Lester et al, J. Fluid Mech. (2022)

- 3D isotropic Darcy flow has Lagrangian kinematics similar to two superposed 2D Darcy flows

3D Steady Anisotropic Darcy Flow

$$\mathbf{F}'(t) = \begin{pmatrix} F'_{11} & F'_{12} & F'_{13} \\ 0 & F'_{22} & F'_{23} \\ 0 & 0 & F'_{22} \end{pmatrix}$$

- 3D anisotropic Darcy flow: $\mathbf{v}(\mathbf{x}) = -\mathbf{K}(\mathbf{x}) \cdot \nabla\phi(\mathbf{x})$

$$\mathbf{K}(\mathbf{x}) = \begin{pmatrix} K_{11}(\mathbf{x}) & 0 & 0 \\ 0 & K_{22}(\mathbf{x}) & 0 \\ 0 & 0 & K_{33}(\mathbf{x}) \end{pmatrix}$$

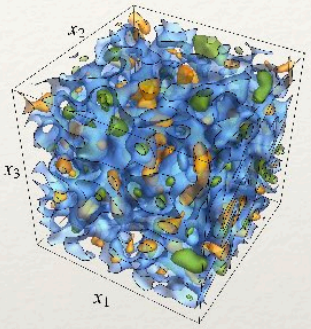

- Helicity non-zero if $K_{ii} \neq K_{jj}$ - braiding of streamlines increases with $\sigma^2_{\ln K}$:

$\sigma^2_{\ln K} = 1$: 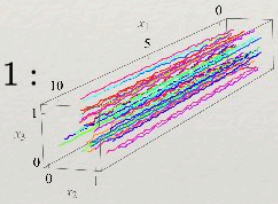

$\sigma^2_{\ln K} = 2$: 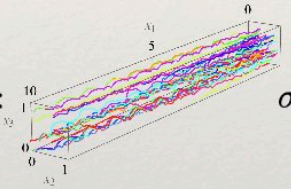

$\sigma^2_{\ln K} = 3$: 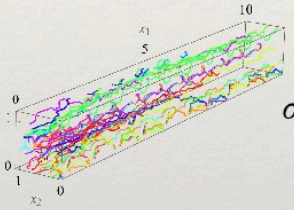

$\sigma^2_{\ln K} = 4$: 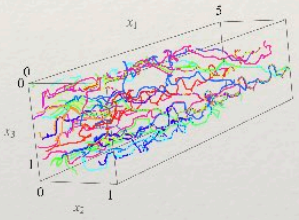

$\ln K_{ii}(\mathbf{x})$ multi-Gaussian fields with variance $\sigma^2_{\ln K}$

- Deformation CTRW: $\langle |F'_{ij}| \rangle = t^r e^{\lambda_\infty t}, \; j > i$

- Lyapunov exponent and transverse dispersivity exactly linearly correlated and grow linearly with heterogeneity:

- Longitudinal and transverse deformation characterised by $\lambda_\infty, \; r$:

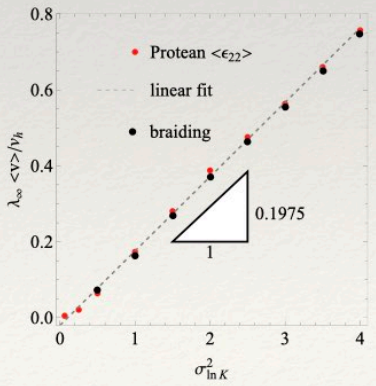

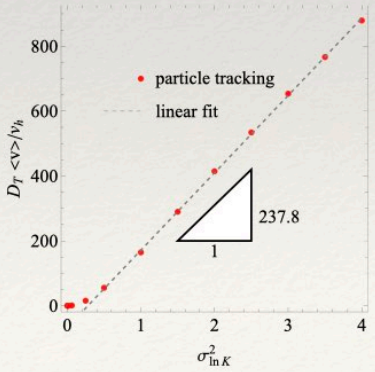

Lester et al, J. Fluid Mech (2018), ArXiV (2023)

7. Deformation in Unsteady Porous Media Flow

Spatio-Temporal Markovianity

- For unsteady flow, velocity can decorrelate in *both* space and time. Consider the steady velocity fields:

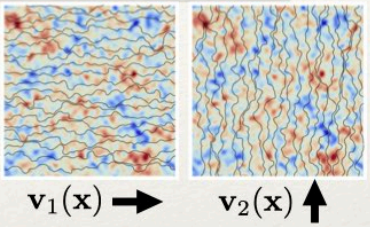

- Unsteady flow via random forcing: $\mathbf{v}(\mathbf{x},t) = f(t)\mathbf{v}_1(\mathbf{x}) + (1-f(t))\mathbf{v}_2(\mathbf{x})$

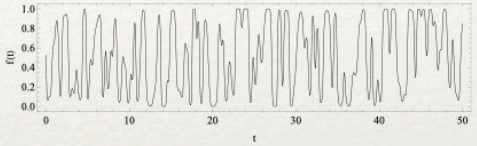

- If s_d, t_d are the decorrelation length, time for $v(s)$ and $f(t)$, then $v(s,t)$ has correlation function: $R(s,t) = e^{-\frac{s}{s_d} - \frac{t}{t_d}}$

- Decorrelation occurs when $r(s,t) \equiv \dfrac{s}{s_d} + \dfrac{t}{t_d} \geqslant 1$, hence velocity is Markovian in *r*-space and supports the CSTRW:

$$r_{n+1} = r_n + 1, \quad s_{n+1} = s_n + \Delta s_n, \quad t_{n+1} = t_n + \Delta t_n \qquad \text{where } \Delta t_n = \frac{s_d}{v_n + s_d/t_d}, \quad \Delta s_n = \frac{s_d v_n}{v_n + s_d/t_d}$$

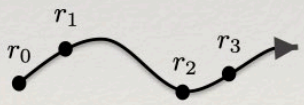

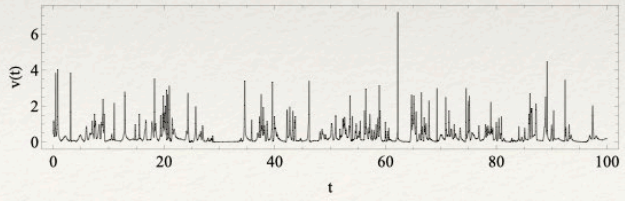

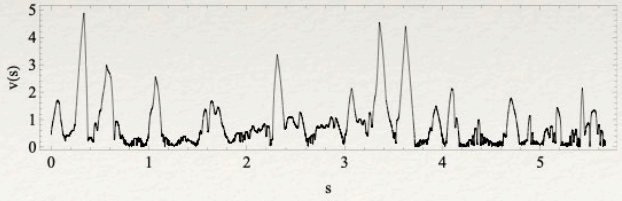

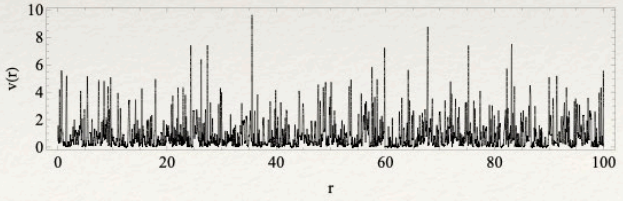

2D Unsteady Darcy Flow

$$\mathbf{F}'(t) = \begin{pmatrix} F'_{11} & F'_{12} \\ 0 & F'_{22} \end{pmatrix}$$

- We can now develop a deformation CTRW for our model flow:
- The *r*-space velocity PDF is related to Eulerian as: $\rho_r(v) = \dfrac{V_r(v)}{\langle V_r \rangle}\rho_e(v),\ V_r(v) = \dfrac{1}{t_d} + \dfrac{v}{s_d}$

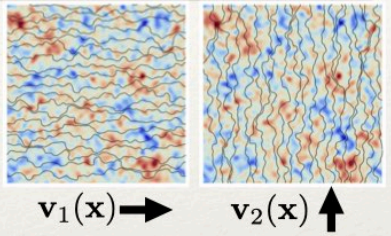

- As $dr = V_r(v)dt$: $F'_{12}(r) = F'_{11}(r)\displaystyle\int_0^r \frac{\epsilon'_{12}(r')F_{22}(r')^2}{V_r(v(r'))}dr' \rightarrow F'_{11}(r)C_1$

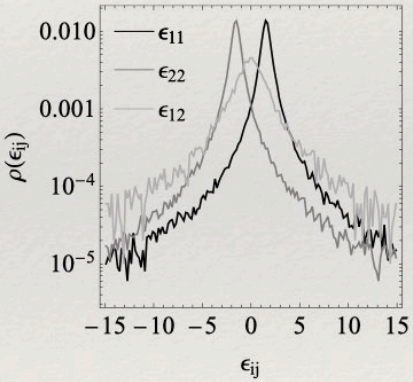

PDFs of $\epsilon'_{ij}(r)$

- Deformation CTRW: $\langle F'_{11}\rangle = \langle F'_{22}\rangle^{-1} = e^{\lambda_\infty t}$ $\qquad \langle |F'_{12}|\rangle = \langle |C_1|\rangle e^{\lambda_\infty t}$

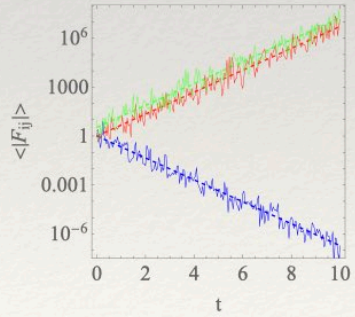

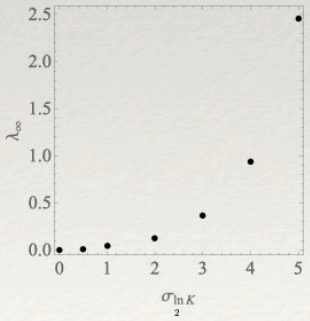

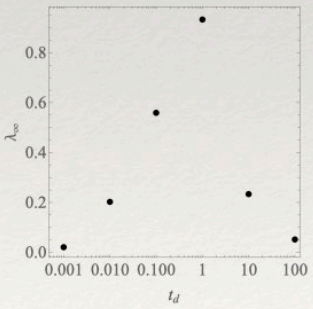

- Deformation governed by Lyapunov exponent, which increases with $\sigma^2_{\ln K}$, exhibits a maximum with t_d

3D Unsteady Pore Scale Flow

- "Push-pull" flow generates heterogeneous and anisotropic dispersion:

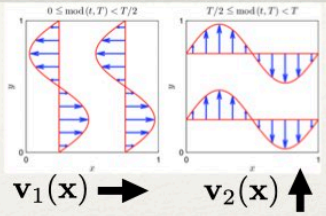

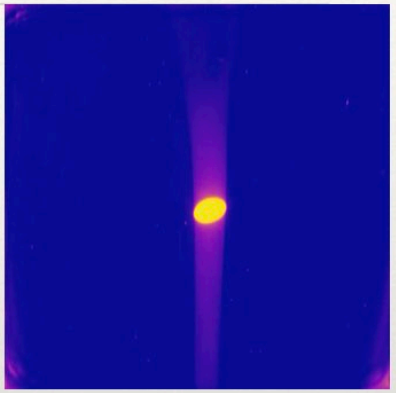

- Similar dynamics for diffusion + reversed time periodic sine flow (RTPSF):

$$\mathbf{v}^*(\mathbf{x},t) = \begin{cases} \mathbf{v}_1(\mathbf{x}) \text{ if } \mathrm{mod}(t,T) < T/2 \\ \mathbf{v}_2(\mathbf{x}) \text{ if } \mathrm{mod}(t,T) > T/2 \end{cases} \qquad \mathbf{v}(\mathbf{x},t) = \begin{cases} -\mathbf{v}^*(\mathbf{x},t) & \text{if } t < T_R \\ \mathbf{v}^*(\mathbf{x}, 2T_R - t) & \text{if } T > T_R \end{cases}$$

- Solute concentration given by particle tracking: $\dfrac{d\mathbf{x}_p}{dt} = \mathbf{v}(\mathbf{x}_p, t) + \sqrt{2D_0}\boldsymbol{\xi}(t) \Rightarrow c(\mathbf{x},t)$

- At $t = T_R$, Eulerian and Lagrangian frames coincide, so push-pull concentration is $c(\mathbf{X}, T_R)$:

- ADE: $\left.\dfrac{\partial c}{\partial T_R}\right|_{\mathbf{X}} = \nabla_{\mathbf{X}} \cdot \left(\mathbf{F}^{-1} \cdot \mathbb{D}_0 \cdot \mathbf{F}^{-\top} \cdot \nabla_{\mathbf{X}} c\right)$ Let $\nu(\mathbf{X},t)$ be leading eigenvalue of $\mathbf{F}^{-1} \cdot \mathbb{D}_0 \cdot \mathbf{F}^{-\top}$:

$c(\mathbf{X}, T_R)$:

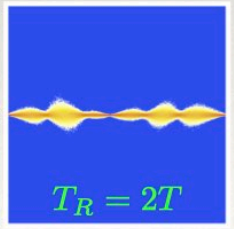

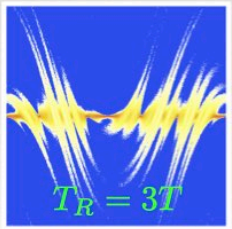

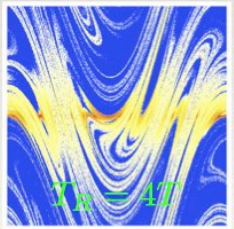

$\nu(\mathbf{X}, T_R)$:

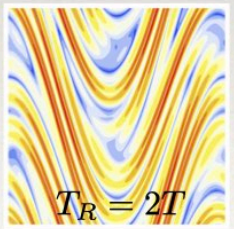

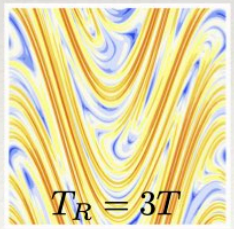

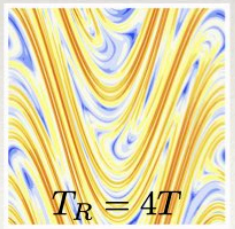

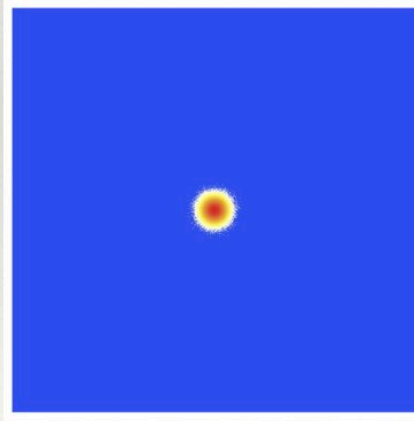

- Deformation controls mixing - connection allows estimation of λ_∞ from experimental $c(\mathbf{x},t)$:

*Heyman et al, Phys. Rev. Lett. (2021)

8. Summary

I: Solute Mixing and Transport

- Solute mixing and transport arises from interplay of *stirring* and *diffusion:*

- Fluid deformation history controls mixing and forms barriers to diffusive transport

- Lagrangian flow structure organises advective transport and mixing:

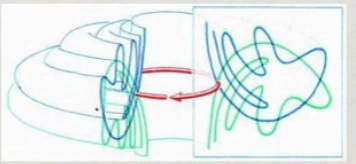

- For periodic and steady flows, classical dynamics uncovers Lagrangian transport: fixed/periodic points, KAM islands, hyperbolic manifolds

- Lagrangian coherent structures govern transport in aperiodic flows; unsteady analogues of classical dynamics

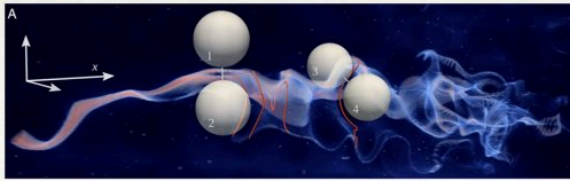

- Chaotic mixing is ubiquitous in steady porous media flows (pore and Darcy scales)

II: Fluid Deformation

- Fluid flow classes span "simple" to "complex" Lagrangian kinematics (LK) - rich datasets now available:

We have developed a stochastic framework that resolves these kinematics:

- Fluid deformation governs mixing - Protean frame quantifies deformation & resolves kinematic constraints
- Deformation across flow classes is characterised by velocity & velocity gradient statistics: $p_v(v)$, $p_{\boldsymbol{\epsilon}'}(\boldsymbol{\epsilon}')$
- Deformation CTRW provides *ab initio* stochastic framework for prediction of deformation: $p_{\mathbf{F}'}(\mathbf{F}')$
- Deformation rates provide inputs for lamellar models of solute mixing & transport: $p_c(c)$

Future challenges:

- Need high-resolution datasets that resolve velocity *and* velocity gradients - robust reconstruction methods
- Further work required linking medium properties to deformation rates

"simple" kinematics

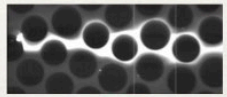

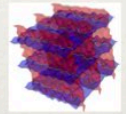

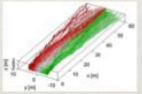

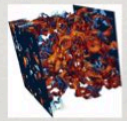

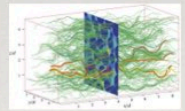

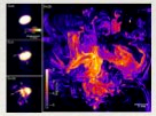

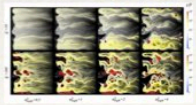

"complex" kinematics

Merci!